The Development of Blood-derived and Lysophosphatidic Acid Containing Scaffolds for Bone Regenerative Applications

PhD thesis book

Aliz Majer PharmD

Doctoral School of Theoretical and Translational Medicine

Semmelweis University

Supervisors: Éva Ruisanchez, MD, Ph.D.
István Hornyák, Ph.D.

Official reviewers: Tímea Feller, PharmD, Ph.D.
Krisztina Ella, MD, Ph.D.

Head of the Complex Examination Committee:

István Karádi, MD, D.Sc.

Members of the Complex Examination Committee:

Henriette Farkas, D.Sc.
Charaf Hassan, D.Sc.

Budapest

2024

1. Introduction

In specific pathophysiological conditions, such as osteoporosis, large bone defects, or certain fractures, the natural healing process of the bone might be compromised. In these conditions, the gap between the bone fragments needs to be filled for proper bone healing. The main objective of Tissue Engineering and Regenerative Medicine (TERM) is to replace, and repair lost or damaged tissues by stimulating the natural regeneration process. Scaffolds are materials that are engineered to contribute to the formation of new functional tissues.

Fibrinogen is a homodimeric glycoprotein, primarily synthesized in hepatocytes and converted into insoluble fibrin, mediated by thrombin, during coagulation. Fibrin is widely used in regenerative medicine, for instance, as a delivery system, as an adhesive during surgeries, in wound healing, or for bone repair. Due to its biocompatibility, controllable biodegradability, cell attachment-promoting properties, and growth factor content, it is also suitable for tissue engineering as a three-dimensional scaffold.

Lysophosphatidic acid (LPA) is a naturally occurring bioactive glycerophospholipid. In the serum LPA is found mainly bound to serum albumin, the main extracellular LPA binding protein. Under physiological conditions, osteoblast-produced LPA is present in bone tissue, and under some pathophysiological conditions, such as fracture healing, bone cells are exposed to high levels of platelet-derived LPA. In different bone cells, LPA induces various cellular effects, including proliferation, differentiation, survival, and migration. Furthermore,

LPA contributes to angiogenesis which is also a key step during the bone regeneration process. Due to these effects, LPA is a promising candidate for applications in bone regeneration.

2. Objectives

Although tissue engineering and regenerative medicine is a highly investigated, emerging field, tissue and organ repair still represents a clinical challenge. The overall aim of our research is the development of a soft tissue implant sufficient for bone regenerative application. The two types of implants we aimed to test during development are injectable, fibrin-containing membranes and freeze-dried, human serum albumin-bound lysophosphatidic acid-coated demineralized bone matrices (DBM). In the experiments, we aimed to investigate if these scaffolds are suitable for further *in vivo* utilization.

First of all, in our experiments, we aimed to prepare fibrin membranes from fresh frozen plasma and different concentrations of cryoprecipitate samples, and intended to investigate if the fibrin membranes are favorable for cell attachment.

Furthermore, we aimed to assess the complex formation between human serum albumin (HSA) and LPA in aqueous solutions for subsequent DBM preparation.

In addition, we intended to determine the effect of the most abundant, albumin-bound 16:0, 18:1, and 18:2 LPA species on the proliferation and migration of human bone marrow-derived mesenchymal stem cells (hBM-dMSCs). Furthermore, we planned to evaluate the biocompatibility and cell attachment capacity of LPA- and HSA-coated DBMs *in vitro*.

3. Methods

Cryoprecipitate samples with different concentrations were isolated from fresh frozen plasma (FPP). The most concentrated cryoprecipitate sample was marked as C4, followed by C3, C2, and C1 with increasing dilution. Sn4, Sn3, Sn2, and Sn1 supernatants were collected from above the precipitate. Platelet-, and red blood cell number, leukocyte, fibrinogen, hemoglobin, albumin, and total protein concentrations, and alkaline phosphatase (ALP) enzyme activity of control plasma and cryoprecipitate were quantitatively determined. Fibrin membranes were isolated from plasma (Control), cryoprecipitate (C1, C2, C2, and C4), and pooled supernatant (Sn). The membranes were freeze-dried, and their weights were measured. Human bone marrow-derived mesenchymal stem cells (hBM-dMSCs) were seeded on fibrin membranes. Live-dead staining was performed after seven days to visualize the attached cells. In addition, the attached cells were quantified with cell proliferation XTT assay.

The complex formation between LPA and HSA was analyzed with Fourier-transform infrared (FTIR) spectroscopy. FTIR spectra of HSA-bound LPA species were compared to native HSA. The effect of the most abundant 18:1, 18:2, and 16:0 LPA species on the proliferation, and migration of hBM-dMSCs was investigated. Cortical bone pieces were harvested from the parietal bone of adult C57Bl/6 mice, and demineralized bone matrices (DBMs) were prepared. DBMs were coated with either 18:2 LPA, HSA, or 18:2 LPA and HSA in combination. The cell attachment capacity of coated DBMs was measured. All data are presented as mean ± SEM.

4. Results

The number of cellular elements was measured in cryoprecipitate with different concentrations, supernatants, and control plasma. In plasma, a small number of platelets, leukocytes, and red blood cells were found in the samples (Figure 1). Platelets were also present in cryoprecipitate samples, and their number was directly proportional with the cryoprecipitate concentration (Figure 1A).

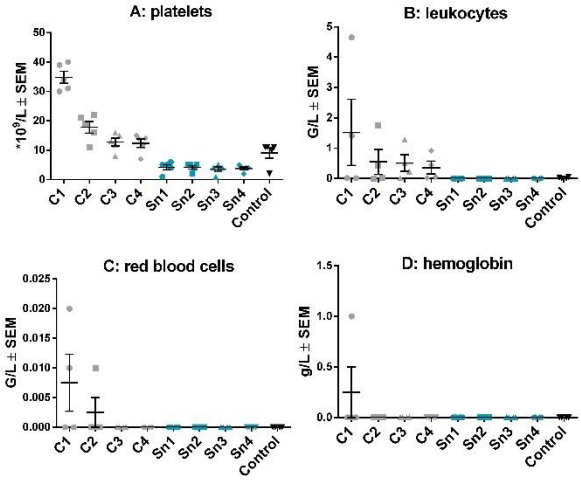

Figure 1. *Platelet (A), leukocyte (B), red blood cell (C), and hemoglobin (D) content of different plasma-derived samples.*

The protein content measurements showed that cryoprecipitate with higher concentrations contained more fibrinogen (Figure 2A). The control sample concentration was approximately 2.5 g/L, which amount was multiplied in the case of C1 (on average 6.5 g/L). The total protein concentration was also slightly affected by cryoprecipitate isolation (Figure 2C). Albumin was detected in the

samples with approximately 40 g/L concentration; however, the tendency of decreasing albumin concentration with decreasing cryoprecipitate concentration is not clear (Figure 2D). ALP activity was also measurable in the examined samples, but no significant difference was observed (Figure 2B).

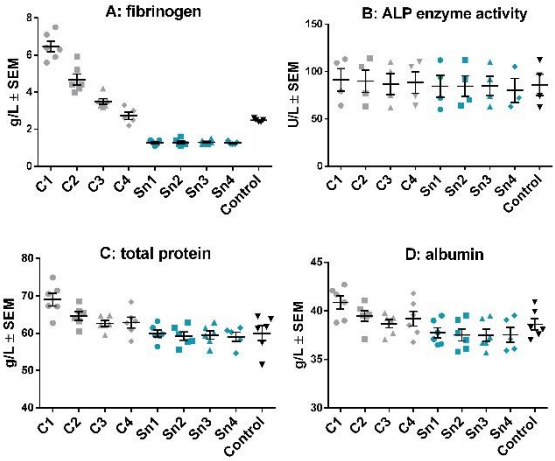

Figure 2. *Fibrinogen (A), total protein (C), albumin (D) content, and ALP enzyme activity (B) of different cryoprecipitate groups.*

Weight measurement of freeze-dried fibrin membranes with different thicknesses showed that every membrane isolated from cryoprecipitate samples had significantly higher weight compared to the control group (Figure 3).

According to the live-dead staining of hBM-dMSCs on fibrin membranes, the cell distribution on the membranes' surfaces was not homogenous; preferred regions with more cells can be seen in the images. Based on the microscopic images, the fibrin membrane

thickness does not influence the scaffold's cell attachment capacity (Figure 4).

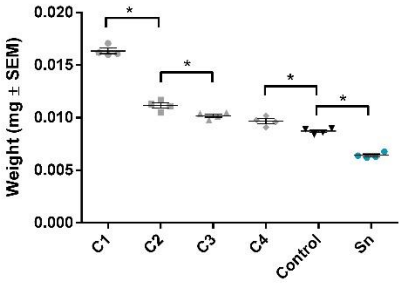

Figure 3. *Weights of freeze-dried fibrin membranes* (*p<0.05, n=4 in each group).

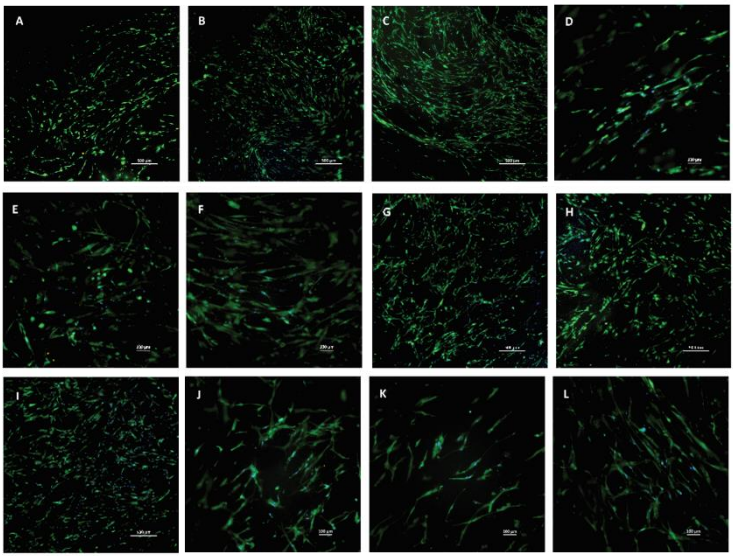

Figure 4. *Live-dead staining of hBM-dMSCs cultured on different fibrin membranes.* Live cells are shown in green, dead cells in yellow, and nuclei are blue. Images were taken at 4× (A-C), and (G-I), or at

10× (D-E) and (J-L) magnification and the scale bars represent either 500 (A-C, and G-I) or 100 (D-F, and I-L) μm. The fibrin membrane groups, isolated from cryoprecipitate, are the following: C1 (A, D); C2 (B, E); C3 (C, F); C4 (G, J); Sn (H, K); and Control (I, L).

Quantitative measurements of cell attachment and viability on fibrin membranes showed no significant difference between the examined groups (Figure 5).

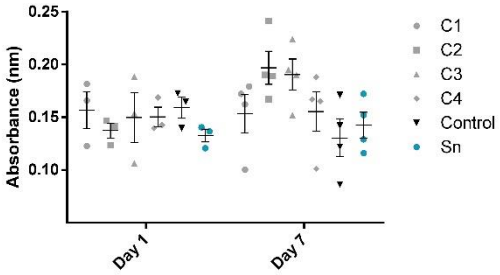

Figure 5. The viability of hBM-dMSCs cultured on the fibrin membranes. Cell attachment after one day and cell proliferation after seven days of culture on fibrin membranes (n = 3 on day 1 and n = 4 on day 7).

FTIR analyzes showed slight spectral shifts of the characteristic amide I (1648 cm^{-1}) and amide II (1537 cm^{-1}) bands of albumin when administered in the presence of LPA. The spectral shift was 1 cm^{-1} in the case of albumin-bound 18:1 LPA and 3 cm^{-1} in the case of 18:2 and 16:0 LPA variants (Figure 6).

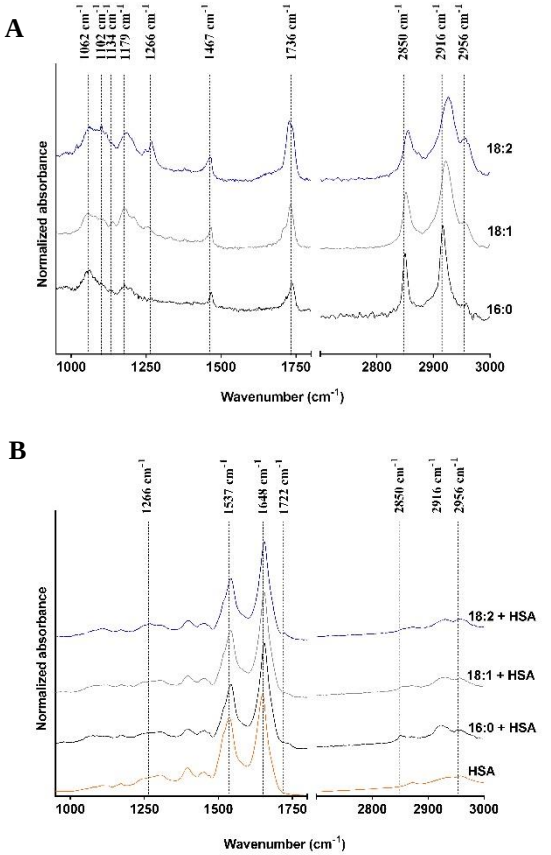

Figure 6. *FTIR spectra of native and HSA-bound LPA species and native HSA.* Native 16:0 LPA is shown at the bottom, 18:1 in the middle, and 18:2 at the top of the image (A). The bottom line shows the FTIR spectra of native HSA and, in a vertical sequence, HSA-bound 16:0, 18:1, and 18:2 LPA species are shown (B).

We performed XTT measurements to investigate the possible cytotoxicity and to determine the effects of 18:1, 18:2, and 16:0 LPA

on the proliferation of hBM-dMSCs. After 24 h of treatment, none of the three LPA species showed cytotoxic effects up to 10 µM concentration, and the different LPA species enhanced cell proliferation dose-dependently when administered in combination with HSA (Figure 7). Interestingly, among the examined three LPA species, only 18:2 LPA in 3 and 10 µM concentrations significantly increased cell proliferation when administered without HSA (Figure 7B).

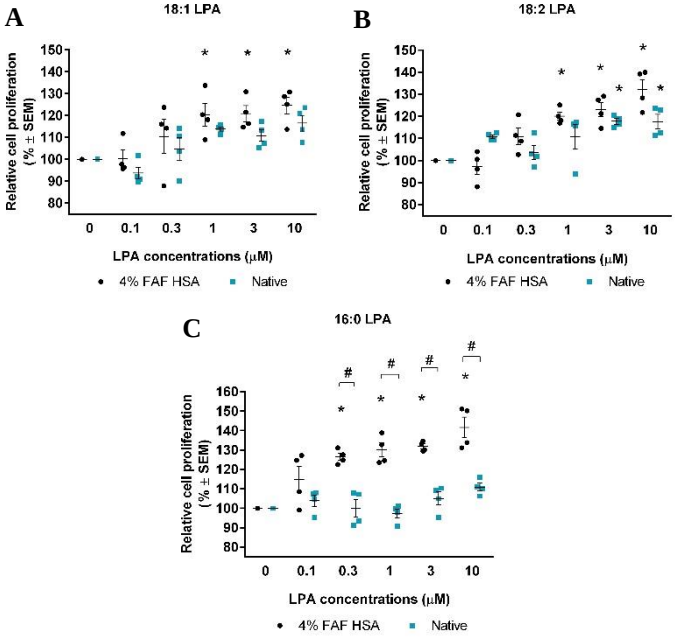

Figure 7. *The effect of LPA species on hBM-dMSCs proliferation.* Relative cell proliferation after 18:1 (A), 18:2 (B) and 16:0 (C) LPA treatment in combination with HSA (4% FFA HSA, black dots) or

alone (native, blue squares). (* $p < 0.05$ vs. Control (0 µM LPA), # $p < 0.05$, n = 4 in each group).

None of the three LPA species significantly enhanced cell migration, neither 12 h nor 24 h after treatment, compared to the control group. There was also no remarkable difference between the HSA-bound LPA and the native LPA-treated groups (Figure 8).

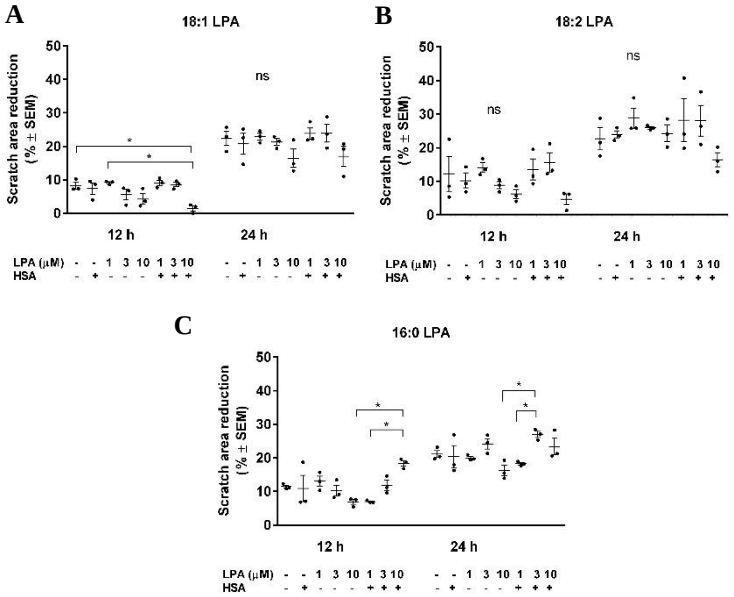

Figure 8. *Scratch area reduction (%) after treatment with (A) 18:1, (B) 18:2 and (C) 16:0 LPA species for 12 and 24 h*. hBM-dMSCs were treated with different LPA species in 1 µM, 3 µM, and 10 µM concentrations alone or combination with HSA (* $p < 0.05$, n = 3).

Attachment of hBM-dMSCs was examined on differently coated DBMs after one day and seven days of incubation. The results show

that cells attached to the surface of bone grafts in every group, but no significant difference was observed between the groups after one day and seven days either (Figure 9).

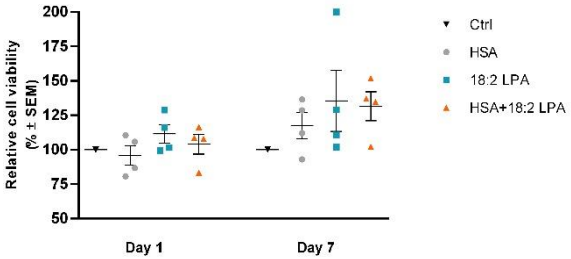

Figure 9. *Relative viability of hBM-dMSCs seeded on different DBMs after one and seven days of incubation.* DBMs were coated with either PBS (Ctrl), HSA, 18:2 LPA, or HSA and 18:2 LPA together (n=4 in each group).

5. Conclusions

According to our results, it can be concluded that plasma products with increased fibrinogen and platelet concentration can be efficiently prepared from cryoprecipitate. At the same time, the level of the other measured components remained mainly similar. Fibrin membrane thickness increased with the increasing fibrin concentration of the membranes, which is favorable regarding TERM-related applications. Microscopic analysis revealed that fibrin membranes are convenient for stem cell attachment, which is a necessary factor for proper scaffold implantation and one of the most important criteria of scaffold development. Quantification of the hBM-dMSCs attachment with XTT assay showed no significant difference between the various fibrin membrane groups, which indicates that membrane thickness does not influence the degree of cellular attachment or proliferation.

The FTIR results prove that complex formation occurs between the components in an aqueous solution; thus, HSA can be used as a potential carrier for LPA in our further experiments. From cell viability measurement data, we concluded that the investigated 16:0, 18:1, and 18:2 LPA species are safe to be used up to 10 μM concentration due to their non-toxic characteristics in hBM-dMSCs. Furthermore, LPA promoted cell proliferation dose-dependently, in combination with HSA. Cell viability and proliferation results showed that 18:2 LPA in 10 μM concentration was the most effective either when administered alone or in the presence of HSA. Therefore, it seems to be a promising supplementation in TERM-related applications. Cell migration analysis showed no remarkable

enhancement after LPA treatment, with or without HSA. Thus, it can be said that the observed cell proliferative effect of LPA treatment is not directly in connection with the enhanced migration of hBM-dMSCs.

The *in vitro* analysis of fibrin membranes and supplemented DBMs showed that both scaffolds might be suitable for in vivo application. However, regarding bone regeneration, 18:2 LPA and HSA-coated DBMs seem to be the most promising candidates due to their high biocompatibility and hBM-dMSCs viability and proliferation-promoting properties. Our experiments might contribute to the development of a new, more effective, innovatively manufactured bone replacement product that enables faster and superior regeneration, thus shortening healing time and lowering the risk of further injuries.

6. Bibliography of the candidate's publications

Publications related to the dissertation

Majer A, Pesthy J, Besztercei B, Hinsenkamp A, Smeller L, Lacza Z, Benyó Z, Ruisanchez É, Hornyák I. Characterization of Native and Human Serum Albumin-Bound Lysophosphatidic Acid Species and Their Effect on the Viability of Mesenchymal Stem Cells In Vitro. Applied Sciences. 2022;12(16):8183. **IF: 2.7**

Hinsenkamp A, Kun K, Gajnut F, **Majer A**, Lacza Z, Hornyák I. Cell Attachment Capacity and Compounds of Fibrin Membranes Isolated from Fresh Frozen Plasma and Cryoprecipitate. Membranes (Basel). 2021;11(10). **IF: 4.2**

Other publications

Hinsenkamp A, Fülöp Á, Hricisák L, Pál É, Kun K, **Majer A**, Varga V, Lacza Z, Hornyák I. Application of Injectable, Crosslinked, Fibrin-Containing Hyaluronic Acid Scaffolds for In Vivo Remodeling. J Funct Biomater. 2022;13(3). **IF: 4.8**

Janovicz A, **Majer A**, Kosztelnik M, Geiszt M, Chun J, Ishii S, Tigyi G, Benyó Z, Ruisanchez É. Autotaxin-Lysophosphatidic Acid Receptor 5 Axis Evokes Endothelial Dysfunction via Reactive Oxygen Species Signaling. Experimental Biology and Medicine. 2023; **IF: 3.2**

Cumulative impact factor of the candidate's publications: **15.262**